Computational analysis of flowering in pea (*Pisum sativum*)

Bénédicte Wenden[1], Elizabeth A. Dun[2,3], Jim Hanan[2,4], Bruno Andrieu[5], James L. Weller[6], Christine A. Beveridge[2,3] and Catherine Rameau[1]

[1]INRA, Institut JP Bourgin, UR 254 Station de Génétique et d'Amélioration des Plantes, 78026 Versailles, France; [2]The University of Queensland, Australian Research Council Centre of Excellence for Integrative Legume Research, St. Lucia, Qld 4072, Australia; [3]The University of Queensland, School of Biological Sciences, St. Lucia, Qld 4072, Australia; [4]The University of Queensland, Centre for Biological Information Technology, St. Lucia, Qld 4072, Australia; [5]INRA, UMR 1091 Environnement et Grandes Cultures, 78850 Thiverval-Grignon, France; [6]School of Plant Science, University of Tasmania, Hobart, Tas. 7001, Australia

Author for correspondence:
C. Rameau
Tel: +33 130833289
Email: rameau@versailles.inra.fr

Received: *3 March 2009*
Accepted: *7 May 2009*

New Phytologist (2009) **184**: 153–167
doi: 10.1111/j.1469-8137.2009.02952.x

Key words: flowering, long-distance signals, modelling, photoperiod, *Pisum sativum*.

Summary

• During plant development, the transition from a vegetative to reproductive state is a critical event. For decades, pea (*Pisum sativum*) has been used as a model species to study this transition. These studies have led to a conceptual, qualitative model for the control of flower initiation, referred to as the 'classical' model. This model involves many inputs, namely photoperiod, genetic states and two mobile signals which interact to determine the first node of flowering.

• Here, we developed a computational model based on the hypotheses of the classical model. Accordingly, we converted qualitative hypotheses into quantitative rules.

• We found that new hypotheses, in addition to those already described for the classical model, were required that explicitly described the signals. In particular, we hypothesized that the key flowering gene *HR* interacts with the photoperiod pathway to control flowering. The computational model was tested against a wide range of biological data, including pre-existing and new experimental results presented here, and was found to be accurate.

• This computational model, together with ongoing experimental advances, will assist future modelling efforts to increase our understanding of flowering in pea.

Abbreviations: *DNE*, *DIE NEUTRALIS*; *FD/FT*, *FLOWERING LOCUS D/T*; FS, flowering signal; *GI*, *GIGAS*; *HR*, *HIGH RESPONSE TO PHOTOPERIOD*; *LF*, *LATE FLOWERING*; NFI, node of flower initiation; *PPD*, *PHOTOPERIOD*; RE, relative error; *SN*, *STERILE NODES*; TF, duration from sowing to first flower; *TFL1*, *TERMINAL FLOWER1*.

Introduction

The decision of when to flower is of major importance to plant species, contributing to both reproductive fitness and yield. This decision is regulated by complex signalling networks that integrate environmental and endogenous factors which, together, determine the time of flowering (Boss *et al.*, 2004). Since the early 1950s, garden pea (*Pisum sativum*) has been used as a model species to study the genetic control of flowering time. This is because of the availability of many flowering mutants and the natural variation in flowering time between different wild-type pea cultivars (Murfet & Reid, 1993). This natural variation in flowering time has since been attributed to naturally occurring allelic variation in genes controlling the transition to flowering, for which mutants are also available (King & Murfet, 1985; Taylor & Murfet, 1993, 1996; Arumingtyas & Murfet, 1994; Beveridge & Murfet, 1996).

Pea displays an indeterminate shoot growth habit and, once flowering is initiated at a specific node, termed the first node of flower initiation (NFI), all subsequent later formed nodes are floral. When the plant undergoes the transition to flowering, flowers are initiated with the node in the apex. Consequently, the time of initiation of the first flowering node is considered

to be the time of floral induction. We define the flowering node as the lowest node bearing a fully developed flower, and the NFI as the lowest node bearing an initiated flower which may or may not develop fully (Truong & Duthion, 1993). In this work, we focused on the NFI.

Many studies have been conducted to identify potential signalling pathways controlling flowering time in pea, including the physiological characterization of flowering mutants grown in different environmental conditions (for example, long-day or short-day photoperiods) and grafting studies (reviewed in Weller *et al.*, 1997). Environmental factors, including vernalization and photoperiod, are important regulators of flowering time in pea (Reid *et al.*, 1996; Weller *et al.*, 1997), the latter being the most studied. For example, a wild-type pea plant (which is a long-day plant) flowers earlier when grown under long-day conditions, and its flowering time is highly sensitive to changes in photoperiod.

Natural variation in the flowering time of different pea cultivars, defined by the NFI on the main shoot of the plant, have been classified phenotypically (Murfet, 1977). This natural variation was found to be caused by variation in the main flowering loci: *SN* (*STERILE NODES*), *LF* (*LATE FLOWERING*) and *HR* (*HIGH RESPONSE TO PHOTOPERIOD*) (Murfet, 1971b, 1973). Subdivision into classes of NFI has been useful to elucidate the genetic basis of flowering differences. NFI is usually within the range of nodes 7–8 for the very early initiating genotypes (Murfet, 1977), and nodes 9–16 for the early initiating genotypes (Murfet, 1971a). After the identification of loci controlling the response to photoperiod, the day-neutral class was defined. Day-neutral plants are very early flowering, but the NFI is not changed by the photoperiod (for example, *sn*; King & Murfet, 1985). In the late classes, the flowering time and NFI are delayed by short-day photoperiods with NFI usually in the range of nodes 14–40 (Murfet, 1971a). Plants that flower late but are highly responsive to photoperiod, whereby flowering is dramatically delayed in short days, generally have an NFI in the range of nodes 20–60 (for example, *Hr*; Murfet, 1973).

For several decades, a descriptive, qualitative model for the regulation of flowering in pea has been used to explain how environmental and genetic factors control the NFI (reviewed in Weller *et al.*, 1997). This model, based on physiological experiments conducted over the past 30 yr, is herein referred to as the 'classical' model. In this model, two graft-transmissible signals are synthesized in the leaves and move towards the apex to regulate the transition to flowering. These signals are a flowering inhibitor produced by a system of three genes, *SN* (Barber & Paton, 1952; Murfet, 1971c; Murfet & Reid, 1973), *DNE* (*DIE NEUTRALIS*) (King & Murfet, 1985) and *PPD* (*PHOTOPERIOD*) (Taylor & Murfet, 1996), and a flowering stimulus that is dependent on the gene *GI* (*GIGAS*) (Beveridge & Murfet, 1996) (Fig. 1a). The transition to flowering is triggered when the flowering signal, which is defined by the ratio of the flowering stimulus to the flowering inhibitor, exceeds a certain threshold (Murfet, 1971a,c).

As mentioned above, *HR* and *LF* are also known to play important roles in the regulation of the transition to flowering in pea. The *HR* gene has little effect in long-day photoperiods, but dramatically delays flowering time, and hence increases NFI, in short-day photoperiods (Murfet, 1973). *LF* is a dominant gene involved in the determination of the lowest possible NFI (Murfet, 1971a,c). Four main naturally occurring alleles of *LF* have been identified, *lf-a*, *lf*, *Lf*, *Lf-d*, each with increasing dominance conferring increasing NFI and hence delaying the time of flowering (Murfet, 1975, 1977). The action of *LF* is not graft transmissible, and it has been proposed that *LF* operates at the apex to determine the minimum level, or threshold, of the flowering signal required to induce flower initiation (Murfet, 1989).

Different approaches have been used to study the regulation of flowering time in pea. The duration from sowing to first flower (TF) and the rate of progress from sowing to flowering (1/TF) have been found to show a linear relationship to the mean temperature and photoperiod (Berry & Aitken, 1979; Alcalde *et al.*, 1999a, 2000). These relationships were directly related to the *LF*, *SN* and *HR* genotypes (Berry & Aitken, 1979; Alcalde *et al.*, 2000). By observing responses to photoperiod and temperature, Alcalde *et al.* (1999b) could predict the *SN*, *LF* and *HR* genotypes for cultivars with unknown genotypes. However, these models do not describe the underlying genetic signalling network.

As proposed, the classical model for the regulation of NFI in pea was successful in providing a scheme to interpret experimental results. However, although the classical model describes the trends of flowering behaviour based on genotype and environmental conditions, it does not provide a precise, quantitative NFI.

Research in biological sciences is turning to mathematical and computational approaches to help solve complex problems (for example, Bayliss, 1902; Mendoza & Alvarez-Buylla, 2000; Espinosa-Soto *et al.*, 2004; Heisler & Jönsson, 2006; Kramer, 2006), because it allows the rigorous testing of hypotheses. Some mechanistic models of plant development incorporate genetic regulatory networks, such as those controlling flower morphogenesis and root hair development in *Arabidopsis* (*Arabidopsis thaliana*; Mendoza *et al.*, 1999; Mendoza & Alvarez-Buylla, 2000; Espinosa-Soto *et al.*, 2004; Chaos *et al.*, 2006). There are also examples of qualitative genetic networks that have been converted into quantitative predictive tools, such as that of Welch *et al.* (2003), which predicts flowering time under the control of seven genes and temperature in *Arabidopsis*.

Our aim was to use a computational modelling approach to test whether the classical model for flowering regulation in pea, based on the wide set of genetic and phenotypic data, accurately accounts for all NFI data. This work should provide a basis for further modelling analyses and should, in the future, facilitate the integration of new molecular data (for

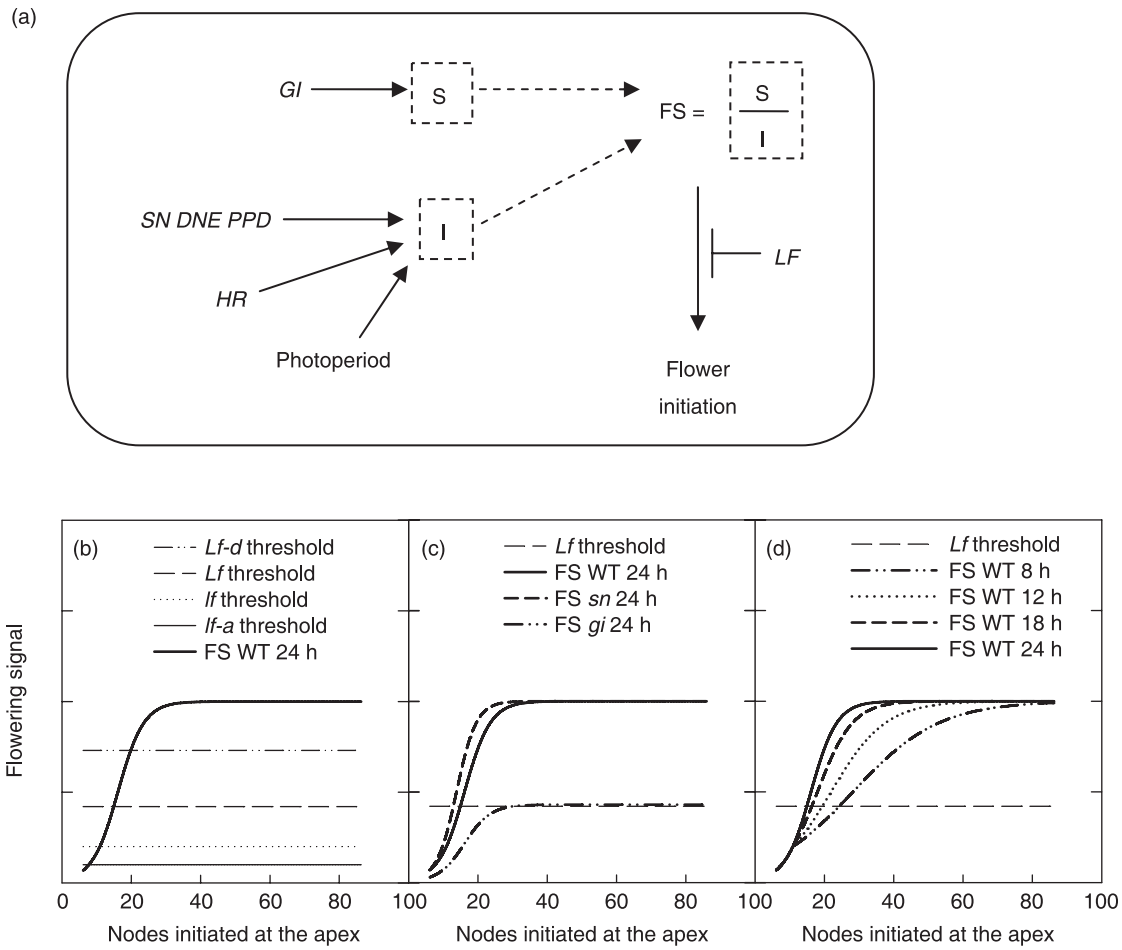

Fig. 1 Classical model for the regulation of flowering node in pea (*Pisum sativum*). (a) Schematic representation of the control of flowering in pea: a mobile flowering inhibitor (I) and mobile flowering stimulus (S) are integrated as a flowering signal (FS), which is equal to the ratio S/I. Flowering occurs when FS exceeds a certain threshold defined by the allele for *LF*. Signals are under genetic and photoperiod control (mobile signals are indicated with broken lines, and genes in italic). Arrowheads indicate promotion, and flat-ended lines represent repression. (b, c, d) Based on the classical model hypothesis, the computational model simulates the level of FS over time. Flowering is triggered when FS reaches the flowering threshold, which is defined by the *LF* allele (*lf-a*, *lf*, *Lf*, *Lf-d*; represented by horizontal lines). (c, d) Change in the level of FS as nodes are initiated at the apex in *sn* and *gi* mutants grown in a 24-h photoperiod (c) and in the wild-type (WT) grown under different photoperiods (d). WT has the genotype (*SN GI hr*). *DNE*, *DIE NEUTRALIS*; *GI*, *GIGAS*; *HR*, *HIGH RESPONSE TO PHOTOPERIOD*; *LF*, *LATE FLOWERING*; *PPD*, *PHOTOPERIOD*; *SN*, *STERILE NODES*.

example, Foucher *et al.*, 2003; Hecht *et al.*, 2005, 2007). In the literature, NFI is usually reported, but the time of floral initiation is not. Consequently, we designed our computational model to predict the NFI rather than the time of floral initiation. In this work, prediction of the NFI is achieved by solving equations that are based on hypotheses describing the interaction of genotype and photoperiod in the regulation of NFI in pea. This allowed us to assess quantitatively whether one set of hypotheses could explain all NFI experimental results for different pea lines grown under different photoperiods. Although the NFI for many different genotypes grown under different photoperiod conditions have been reported previously, some genotype–environment interactions have not been tested as yet, particularly for genotypes with the dominant allele *Hr*. Accordingly, to examine these genotype–environment interactions, we conducted experiments to determine the NFI for different genotypes grown in different photoperiods.

In this paper, the general principles and components of the mathematical model are first described, leading to the initial expression of the classical model for the regulation of NFI in a quantitative form. The hypotheses of the classical model are complemented by new hypotheses that were necessary to build the computational model. In particular, new hypotheses were required to specify the effects of the interaction between the *HR* genotype and photoperiod on NFI. The computational model was refined, fitted and evaluated against a wide range of NFI data, including already published and new experimental results. Finally, perspectives for model application and the ability to integrate new data are discussed.

Model description

General principles

The hypotheses on the regulation of NFI in pea, developed by Murfet and colleagues, described two signals and the genes controlling the production of these signals (Murfet, 1989; Beveridge & Murfet, 1996; Weller *et al.*, 1997). In this work, we propose what we believe to be the simplest way to model the classical hypotheses for the effect of genotype and photoperiod on NFI in pea. The proposed equations quantify the level of signals in different genotypes and photoperiods. Because the true nature of these signals have not yet been elucidated, our modelling approach is not based on their quantification or on the fine regulation of gene expression and protein translation, such as that used in circadian clock modelling (e.g., Locke *et al.*, 2005). Rather, we have modelled the hypothetical signal levels in the whole plant, based on the hypotheses. Although grafting studies have demonstrated that the signals are produced and perceived in different locations (leaves and apex, respectively), we assume here that signal transport takes place at a rate sufficiently fast such that no significant delay occurs between production and perception. Accordingly, our modelling approach represents the plant as one fully integrated entity. The model can be used to determine the NFI for different genotypes grown in photoperiods ranging from 8 to 24 h.

In pea, temperature affects flowering time via the rate of leaf initiation and emergence, but does not affect the NFI (Truong & Duthion, 1993). As a consequence, in our model, time is expressed in plastochron units from the time of sowing. A plastochron is the physiological time interval separating the initiation of two successive nodes. The number of nodes already initiated in the embryo (within the seed) is described as a model parameter.

The model simulates the concentration of the two mobile signals controlling flowering in pea, the flowering inhibitor (I) and the flowering stimulus (S), over time. The two signals interact to regulate the level of a flowering signal (FS), which increases over time (Fig. 1b). A flowering threshold determines the minimum level of FS necessary to trigger flower initiation (Fig. 1b). The photoperiod and the genotypes of each of the flowering genes (*SN, LF* and *HR*) are defined by the user. Photoperiod affects signal levels (Fig. 1d) according to a function that is dependent on the genotype of the flowering genes (Fig. 1c). In many plant species, a juvenile photoperiod-insensitive phase has been identified (Collinson *et al.*, 1992). That early flowering genotypes do not respond to changes in photoperiod supports the hypothesis that a juvenile stage probably exists in pea. Using grafting experiments, it has been shown that the photoperiod is likely to be perceived by fully expanded leaves (Lang *et al.*, 1977; Colasanti & Sundaresan, 2000). Early versions of the model (data not shown) were unable to predict the flowering behaviour of very early flowering lines, such as *lf-a* plants, until this insensitivity period was incorporated. As such, in the model, the pea plant is insensitive to the photoperiod until the first leaf is open, which corresponds to node 3 (counting cotyledons as node 0 and scale leaves as nodes 1 and 2).

Hypotheses were formulated based on the literature and experiments. They are reported in the results, listed in Table 1, and referred to as hypothesis '#' throughout the text. Three steps were then taken to create the computational model. Firstly, hypotheses were converted to equations, including one ordinary differential equation, describing the rates of change of signal levels. Parameter values were then estimated using optimization methods. Finally, the sensitivity of the model to variations in the constant and parameter values was determined.

Flowering stimulus

The ability of early day-neutral rootstocks to induce early flowering in late photoperiod-responsive scions provided evidence for a graft-transmissible floral stimulus in pea (Haupt, 1969; Murfet, 1971c). The *gi* mutant (Murfet, 1989) flowered later than the wild-type in all conditions tested, and did not flower at all in some conditions (Beveridge & Murfet, 1996). In reciprocal grafts between *gi* and the wild-type, flowering was promoted in *gi* shoots when a wild-type scion or rootstock was present (Beveridge & Murfet, 1996). These results suggest that the *gi* mutation blocks the synthesis of a flowering stimulus. It is therefore hypothesized that the production of a mobile flowering stimulus is mediated by *GI* (Fig. 1a; Table 1; hypothesis 1). As *gi* plants do eventually flower in most conditions, the mutant allele might be leaky, producing some functional product (Beveridge & Murfet, 1996) (Table 1; hypothesis 2).

In the computational model, the flowering stimulus (S) is constant over time, and depends on the genotype at the *GI* locus:

$$S = K_S \times \beta_{GI} \qquad \text{Eqn 1; hypotheses 1, 2}$$

(K_S, quantity of stimulus S in *GI* plants; β_{GI}, genotype parameter, which is equal to unity in the *GI* wild-type with a reduced value in *gi* mutant plants; see Table 2 for values of parameters and constants; see Materials and Methods for parameter estimation).

Flowering inhibitor

Grafting experiments conducted with mutants have provided evidence that the *SN*, *DNE* and *PPD* genes might control steps in a biosynthetic pathway that leads to the production of a flowering inhibitor (I) (Barber & Paton, 1952; Murfet, 1971c; Murfet & Reid, 1973; King & Murfet, 1985; Taylor & Murfet, 1996) (Fig. 1; Table 1; hypothesis 3). For example, mutant *sn* rootstocks promote flowering in wild-type shoots, whereas wild-type rootstocks cause a small delay in flowering

Table 1 Hypotheses used to build the computational model based on the literature and new results

	Hypothesis	Source
Hypotheses based on previous studies		
1	*GI* constitutively promotes the production of a mobile floral stimulus	Haupt (1969); Murfet (1971c); Beveridge & Murfet (1996)
2	The *gi* mutant is a leaky mutant, producing some functional product	Beveridge & Murfet (1996)
3	*SN DNE PPD* system controls the production of a mobile floral inhibitor; the three-gene system is considered as one in the computational model	Barber & Paton (1952); Murfet (1971c); Murfet & Reid (1973); King & Murfet (1985); Taylor & Murfet (1996)
4	The inhibitor level decreases with age	Murfet & Reid (1973); Reid (1979)
5	The production of the inhibitor decreases with increasing day length (photoperiod)	Murfet & Reid (1973); Reid (1979)
6	*SN*, *DNE* and *PPD* genes are all required for the flowering response to the photoperiod	Arumingtyas & Murfet (1994)
7	*HR* acts by maintaining the inhibitor production over time	Murfet (1973); Reid (1979)
8	The flowering signal is the ratio of a flowering stimulus and a flowering inhibitor	Murfet (1971a,c)
9	Flower initiation occurs when the flowering signal (FS) reaches a flowering threshold	Murfet (1971a,c)
10	The flowering threshold is determined by the *LF* allele	Murfet (1971a, 1989)
11	The flowering threshold is constant over time	Murfet (1989)
Hypotheses derived from this study		
12	The number of nodes already initiated in the seed is considered to be constant, independent of genotype and photoperiod, and is equal to 6.4	Table S2 (see Supporting Information)
13	The plant is day length insensitive until it has produced one true expanded leaf (node 3, counting the scales as nodes 1 and 2)	
14	The number of nodes initiated at the apex when node 3 is fully open is considered to be constant and independent of genotype and photoperiod, and is equal to 9.9	Table S5 (see Supporting Information)
15	*HR* interacts with the photoperiod input on the inhibitor synthesis rate	Fig. 2

Table 2 Values of constants and parameters used in the computational model

dt	0.1
K_S	2
I_0	3
K_R	0.05
I_∞	0.2
β_{GI}	1 in *GI* wild-type 0.43 in *gi* mutant
β_{LF}	1 for *lf-a* 2 for *lf* 4.2 for *Lf* 7.3 for *Lf-d*
$\beta_{(SN,HR)}$(photoperiod)	1.3 in *sn* mutant 1 if node ≤ 10 if node > 10: $(-0.0469 + 0.046 \times \text{photoperiod})$ in *hr* plants; $0.0222 \times e^{0.1565 \times \text{photoperiod}}$ in *Hr* plants

dt corresponds to the time step of the model; constants are K_S, the quantity of stimulus S in *GI* wild-type (WT); I_0 and I_∞, the initial and steady-state levels of inhibitor I, respectively; and K_R, the synthesis rate of inhibitor I set for WT at a 24-h photoperiod; β_{GI} and β_{LF} are genotype parameters for *GI* and *LF* genes, respectively; $\beta_{(SN,HR)}$(photoperiod) is the photoperiod function which includes the genotype for *SN* and *HR* as parameters. *GI*, *GIGAS*; *HR*, *HIGH RESPONSE TO PHOTOPERIOD*; *LF*, *LATE FLOWERING*; *SN*, *STERILE NODES*.

in *sn* scions compared with *sn* self-grafts. Grafting results from plants of different ages grown in different photoperiods suggest that the level of I decreases with age (Table 1; hypothesis 4) and long-day photoperiods (Fig. 1; Table 1; hypothesis 5) (Murfet & Reid, 1973; Reid, 1979). Double-mutant analyses have shown that the response to photoperiod in pea is conferred by the joint presence of *SN*, *DNE* and *PPD* (Arumingtyas & Murfet, 1994) (Table 1; hypothesis 6). Mutation in any of the three genes produced a similar early flowering phenotype. Consequently, in this study, *SN*, *DNE* and *PPD* are considered together as a system that is written as '*SN*'.

From grafting experiments, it was concluded that the *HR* gene prevented the decrease in I over time (Fig. 1, Table 1; hypothesis 7) (Murfet, 1973; Reid, 1979), hence delaying NFI in short-day photoperiods (Murfet, 1973).

According to hypothesis 4 (Table 1), the level of I decreases with time in a wild-type plant, from an initial level I_0 to a steady-state level I_∞, as a result of simultaneous processes of synthesis at a constant rate and degradation following first-order kinetics. This was modelled using an ordinary differential equation:

$$\frac{dI}{dt} = r\left(1 - \frac{I}{I_\infty}\right) \qquad \text{Eqn 2a; hypotheses 3, 4, 5}$$

(r, rate of synthesis of I). According to hypotheses 3 and 5 (Table 1), the degradation rate of I is implicitly incorporated in the steady-state I_∞, which corresponds to the ratio between degradation and synthesis. Accordingly, if I_∞ is constant, variations in the synthesis rate r in the model result in variations in the implicit degradation rate. The synthesis rate of I depends on the *SN* genotype and varies with photoperiod:

$$r = K_R \times \beta_{(SN)}(\text{photoperiod}) \qquad \text{Eqn 3a; hypotheses 3, 5, 6}$$

[K_R, synthesis rate of I set for wild-type grown in a 24-h photoperiod; $\beta_{(SN)}$(photoperiod), photoperiod response function (Table 1, hypothesis 5), which includes the genotype of *SN* as a parameter (Table 1, hypothesis 6, see Materials and Methods for estimation of function)].

When r is constant, Eqn 2a has an analytical solution:

$$I(t) = (I_0 - I_\infty)e^{-\frac{r}{I_\infty}t} + I_\infty \qquad \text{Eqn 2b}$$

In addition to this analytical solution, Eqn 2a can be solved numerically. Both solutions are equivalent in the cases analysed here. However, to allow easy modification of the model in future studies, including situations in which the photoperiod, and thus r, would change over time, Eqn 2a was solved numerically in the simulations (see Modelling methods).

The *HR* gene has been suggested to affect the synthesis of I and to be responsible for the high response to photoperiod. However, it is not known whether the effect on the synthesis of I is dependent on photoperiod or whether a simple change in the rate of synthesis of I may result in the high photoperiod response. These two alternative hypotheses are investigated in this study.

Decision to flower

As suggested by Murfet (1971a,c), the flowering signal (FS) is defined as the ratio of the flowering stimulus S to the flowering inhibitor I (Fig. 1; Table 1, hypothesis 8):

$$FS = \frac{S}{I} \qquad \text{Eqn 4, hypothesis 8}$$

Flowering is triggered when FS at the apex exceeds a certain threshold (Table 1; hypothesis 9) (Murfet, 1971a,c). The *LF* allele is hypothesized to define this flowering threshold (Table 1, hypothesis 10) (Murfet, 1989). This threshold remains constant over time (Table 1, hypothesis 11) and is defined by the model parameter β_{LF}, which has a certain value for each *LF* allele (Table 2). Thus, the transition to flowering occurs when FS reaches the β_{LF} threshold. When this occurs, the next node to be initiated at the apex is floral, and therefore is the model-predicted NFI.

Materials and Methods

A wide set of experimental data was necessary to allow parameter estimation for the model. Although numerous data could be obtained from the literature for various genotypes and photoperiod conditions, previous work has not been carried out with a wide range of genotypes under the same photoperiods. In this work, in addition to a summary of the experimental data from the literature, we propose a first real comparison of the flowering behaviours for different genotypes grown under three photoperiods. In order to complete this physiological study, we carried out an analysis on the number of preformed nodes in the embryo for these same various genotypes. Combined, the data obtained from both the literature and new experiments presented here, were used to make and test the computational model.

Biological methods

Plant material Plant material consisted of three wild-type lines (Torsdag, Borek and WL1771) of pea (*Pisum sativum* L.) and flowering mutants for the genes *LF*, *SN*, *DNE* and *HR* obtained in these backgrounds. Mutants *sn-4* (Hecht *et al.*, 2007) and *lf-a* were obtained in a dwarf Torsdag background NGB5839, a derivative of Torsdag carrying the *le-3* mutation (Lester *et al.*, 1999). Mutant lines WL1769 and WL1770 were obtained by fast-neutron treatment of the WL1771 line (Taylor & Murfet, 1993). The genotype of each line is included in Table S1 (see Supporting Information).

Growth conditions For all glasshouse experiments, plants were grown in sand, under natural light extended to a photoperiod of 11, 16 and 20 h by sodium vapour lamps. Nutrient solution was applied to the plants twice a week during the early vegetative phase and then three times a week. The mean glasshouse temperatures were 18.2°C, 18.7°C and 21.7°C, respectively.

Plant measurement To test the effect of genotype and growth conditions of the parent on the number of preformed nodes in the seed, and to calculate the average number of nodes initiated before sowing, seeds of several genotypes from different harvests were dissected. To count the number of

nodes initiated in the embryo, 10 seeds of each genotype were imbibed in water for 24 h and dissected under a microscope (increasing size × 8 to × 40).

Node initiation and leaf appearance on the main stem were recorded. For all genotypes, samples of six plants were collected at 7- to 14-d intervals. Plants were dissected under a microscope (increasing size × 8 to × 40) to determine the state of the apex (vegetative or floral, total number of initiated nodes). The NFI was determined by counting the number of nodes from the first scale leaf (counted as node 1) to the first floral node. In addition, the number of fully expanded leaves was measured on six plants per genotype every 4 d. The open stage of leaves on the main stem was determined on a decimal scale using the nodal stage method of Maurer *et al.* (1966).

Independent experiments were conducted with a range of flowering genotypes and photoperiods to estimate the number of initiated primordia at the apex when the number of open leaves was equal to three, which corresponds to the end of the presumed photoperiod insensitivity phase. The rates of node initiation and the leaf appearance were estimated by linear regression of the counts of primordia and of leaves against time, respectively (Fig. S1, see Supporting Information). The leaf appearance rate was used to determine the time at which the first true leaf (node 3) was open. The number of nodes initiated at the apex at that time was estimated using the node appearance rate.

Modelling methods

Model simulation and parameter estimation were performed using MATLAB 7 (Mathworks, Cambridge, UK). Changes in the levels of signals were modelled using an ordinary differential equation that was solved using Euler's method. The simulation starts with time zero as the time of sowing. At this time, a certain number of nodes are already initiated in the seed and this number was determined experimentally (Table S2, see Supporting Information). The time step was 0.1 of a plastochron.

Parameter estimation and model evaluation The model has several parameters and was fitted to the experimental data by treating some of these parameters as constants. The values of K_S, K_R, I_∞ and I_0 are considered to be independent of environment and genotype, and represent model constants. The model parameters depend on the genotype of the genes *LF* (β_{LF}), *GI* (β_{GI}) and *SN* together with photoperiod [$\beta_{(SN)}$(photoperiod)]. The values for the constants, parameters and functions used in the computational model are shown in Table 2.

β_{LF}, which defines the threshold for FS, can take four increasing discrete values depending on the *LF* alleles (*lf-a*, *lf*, *Lf* and *Lf-d*), following the classification described by Murfet (1975, 1977) (Table 2). β_{GI}, which describes the *GI* genotype, is set to a value of unity in the *GI* wild-type and has a reduced value in *gi* mutant plants (Table 2). $\beta_{(SN)}$(photoperiod), which describes the effect of both photoperiod and genotype for *SN* on I, is equal to a constant value in *sn* mutant plants, and is a function of photoperiod in *SN* wild-type plants (Table 2).

Values of the constants and parameters were estimated by minimizing the relative error (RE) in the prediction of NFI for different genotypes and photoperiods for which there were experimental data to compare, obtained from the literature and new experiments (Table S3, see Supporting Information). RE was calculated by:

$$\mathrm{RE} = \frac{1}{n}\sum_{i=1}^{n}\frac{|O_i - P_i|}{O_i} \qquad \text{Eqn 5}$$

(O_i and P_i, observed and predicted NFI for a given genotype and photoperiod; n, number of genotype × photoperiod combinations). RE was preferred to the root-mean-square error because the experimental variability of NFI within a treatment was found to increase with higher NFI values.

All NFI data for different genotypes and photoperiods, obtained from the literature and experiments (Table S3), were used to estimate the parameters. Several combinations for the constant values were found to minimize RE (data not shown). However, combinations only differed by a scale factor. As such, K_S, the parameter that represents the value of S in *GI* wild-type plants, was arbitrarily set at a value of two, and the scale factor for other parameters presented herein was set accordingly. Experimental data for wild-type (*SN GI hr*) plants grown in a 24-h photoperiod, with β_{GI} and $\beta_{(SN)}$(photoperiod) values equal to unity, were used to estimate the values of constants K_R, I_∞ and I_0.

The values of β_{LF} for the four *LF* alleles, β_{GI} for the *gi* mutant and $\beta_{(sn)}$(photoperiod) for the *sn* mutant were estimated from the NFI for plants grown in a 24-h photoperiod, using the following genotypes: *SN GI hr lf-a/lf/Lf/Lf-d*, *lf sn hr*, *Lf sn hr*, *Lf dne hr*, *Lf ppd hr* and *Lf gi hr*.

The effect of photoperiod on r, the rate of synthesis of I, is expressed through the function $\beta_{(SN)}$(photoperiod) (Eqn 3a). The function $\beta_{(SN)}$(photoperiod) is equal to a constant value $\beta_{(sn)}$(photoperiod) in the *sn* mutant, whereas, in the *SN* wild-type, it varies according to the photoperiod (Table 2). The function was estimated based on NFI data for the genotypes *Lf GI hr*, *Lf gi hr*, *Hr Lf* and *Hr Lf-d* grown in a range of photoperiods, from 8 to 24 h.

The accuracy of the computational model was evaluated by calculating RE in the prediction of NFI (Eqn 5).

Results

Number of nodes preformed in the seed

The number of preformed nodes in the seed was between six and seven (mean 6.4) for a range of genotypes and photoperiods, and was thus independent of growth conditions of the parent

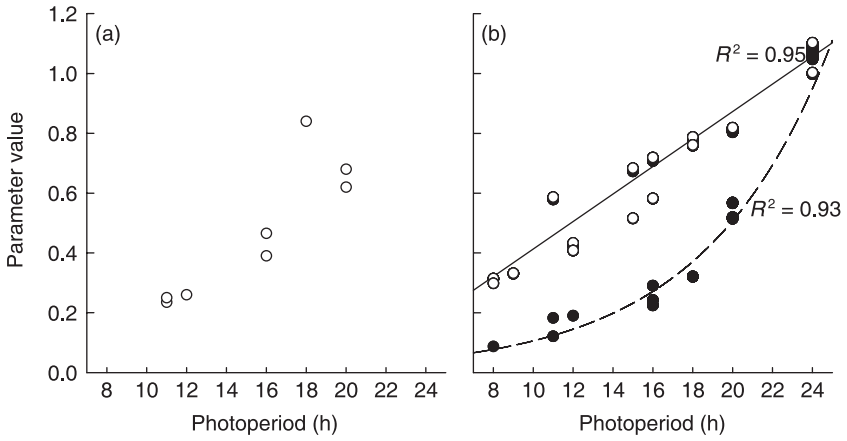

Fig. 2 (a) Estimated values for the *HR* genotype parameter β_{HR} with no photoperiod interaction for *Hr* plants. (b) Estimated values for the photoperiod function $\beta_{(SN,HR)}$(photoperiod). Linear regression (full line) for $\beta_{(SN,hr)}$(photoperiod) function was estimated for *SN hr* plants; exponential regression (broken line) for $\beta_{(SN,HR)}$(photoperiod) function was estimated for *SN Hr* plants. *Hr*, filled circles; *hr*, open circles. *HR*, *HIGH RESPONSE TO PHOTOPERIOD*; *SN*, *STERILE NODES*.

plant (Table S2). The number of preformed nodes in the seed is considered to be a constant in the model, and is accordingly set to 6.4. As a result, the first step of the model corresponds to a physiological age of 6.5 plastochrons (Table 1, hypothesis 12).

Pattern of NFI variations with photoperiod

Data from previous studies (Table S3) and our experiments (Table S4, see Supporting Information) show that early flowering lines (*lf-a*, *lf* and *sn*) flower at a very low node, and do not respond to photoperiod. By contrast, late varieties (*Lf*, *Lf-d*, *gi*) show a response to photoperiod, flowering later when the day length is shorter. Late high-response flowering lines associated with the *Hr* genotype respond dramatically to photoperiod, flowering later than *hr* plants in all conditions, and particularly in short-day photoperiods. This high response is inhibited by early alleles of *LF* (*lf-a* and *lf*).

Photoperiod insensitivity phase

The earliest flowering genotypes show a low NFI independent of photoperiod. Despite being very low, this NFI is still higher than the number of preformed nodes. This suggests that, like other species (Collinson *et al.*, 1992), pea plants experience a juvenile phase in which they are insensitive to day length. We hypothesized that this period extends until one true leaf (node 3, counting the scale leaves as nodes 1 and 2) is fully expanded (Table 1; hypothesis 13). Estimations indicated that an average of 9.9 ± 0.2 nodes are initiated at the apex when the first true leaf opens (Table S5, see Supporting Information). Analysis of variance (ANOVA) indicated that photoperiod had a significant effect on this value (at the 5% level), but with no obvious trend; insufficient data were available to design a regression for the effect. As a result, we used 9.9 as a constant in the model to describe the number of nodes initiated at the apex when the first true leaf opens. Accordingly, in the model, the plant is considered to be insensitive to photoperiod until node 10 is initiated (Table 1; hypothesis 14). This means that, in the computational model, the photoperiod affects the synthesis of I only after node 10 is initiated. Consequently, a basal synthesis rate for I, equal to K_R, is set between sowing and node 10, which corresponds to the native synthesis rate. As the photoperiod does not affect S, FS displays the same evolution over time between nodes 6 and 10 for different photoperiods (Fig. 1d). For very early flowering genotypes (for example, *lf-a*), FS reaches the flowering threshold before the photoperiod affects FS and, consequently, NFI is constant within the range of photoperiods.

Modelling photoperiod and HR effect

The photoperiod action on *r*, which is the rate of synthesis of I, is expressed through the function $\beta_{(SN)}$(photoperiod). In *SN hr* plants, the fitted values of $\beta_{(SN)}$(photoperiod) show a linear behaviour over a range of photoperiods (Fig. 2b, values in Table 2).

HR is hypothesized to affect the production of I (Table 1, hypothesis 7). Two alternative hypotheses that describe the effect of the *HR* gene on the rate of synthesis of I in the model were tested: *HR* affects the production of I independently of photoperiod, and *HR* interacts with photoperiod to affect the production of I.

The hypothesis that *HR* acts on the rate of synthesis of I independent of photoperiod was tested by evaluating whether the *HR* effect could be included through a multiplicative parameter:

$$r = K_R \times \beta_{(SN)}(\text{photoperiod}) \times \beta_{HR}$$

Eqn 3b, hypotheses 3, 5, 6, 7

where *r*, K_R and $\beta_{(SN)}$(photoperiod) are described above, and the value of the genotype parameter β_{HR} depends on the *HR* genotype (Fig. 2a).

The parameter β_{HR} was estimated based on NFI values for *Hr* plants grown in different photoperiods. Estimates of β_{HR} showed a strong dependence on photoperiod (Fig. 2a), making it clear that the effect of *HR* could not be expressed through a single parameter, as proposed in Eqn 3b.

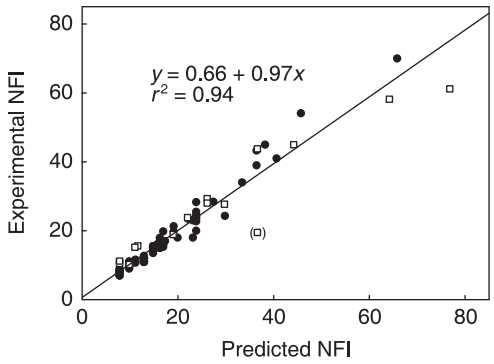

Fig. 3 The node of flowering initiation (NFI) predicted by the computational model fits the experimental data for *hr* (circles) and *Hr* (squares) plants. The data here were used to estimate the parameter values. Symbols in parentheses were not used for the optimization of parameters. *HR*, *HIGH RESPONSE TO PHOTOPERIOD*.

As a single parameter value could not present an accurate estimation of the *HR* effect (Fig. 2a), we considered the other hypothesis that the photoperiod function should include *HR* as a parameter. For *hr* plants, the photoperiod effect is computed through a linear photoperiod function $\beta_{(SN)}$(photoperiod) (Fig. 2b). The photoperiod function $\beta_{(SN,HR)}$(photoperiod) takes into account that the genotype for *HR* affects the photoperiod effect on the synthesis rate of I (Table 1, hypotheses 6 and 7) and, in particular, *HR* interacts with the photoperiod input (Table 1, hypothesis 15):

$$r = K_R \times \beta_{(SN,\,HR)}(\text{photoperiod}) \times \beta_{HR}$$

Eqn 3c, hypotheses 3, 5, 6, 7, 15

[$\beta_{(SN,HR)}$(photoperiod), photoperiod function which includes the genotypes for *SN* and *HR* as parameters].

For short-day photoperiods, the value and rate of change of $\beta_{(SN,Hr)}$(photoperiod) for *Hr* genotypes are lower than for *hr* genotypes (Fig. 2b). However, for *Hr* genotypes under longer photoperiods, $\beta_{(SN,Hr)}$(photoperiod) increases sharply.

We described this behaviour by considering an exponential form for $\beta_{(SN,HR)}$(photoperiod) (Fig. 2b, values in Table 2). Other functions could have been used: for instance, the data are also compatible with a bi-linear behaviour. However, using such a function would require the fitting of three parameters. Our choice reflects the fact that the exponential function could fit the experimental data with only two parameters, which is justified given the limited amount of available data. Accordingly, the values of $\beta_{(SN,HR)}$(photoperiod) that best fitted the experimental NFI data increased exponentially with increasing photoperiod (Fig. 2b, values in Table 2).

The model predictions capture the biological data

As shown in Figs 3 and 4, the model predictions accurately capture the biological data with an RE between the model output and the experimental data of 9%. For *hr* plants, the RE is only 8%. The model is less accurate for *Hr* predictions, as

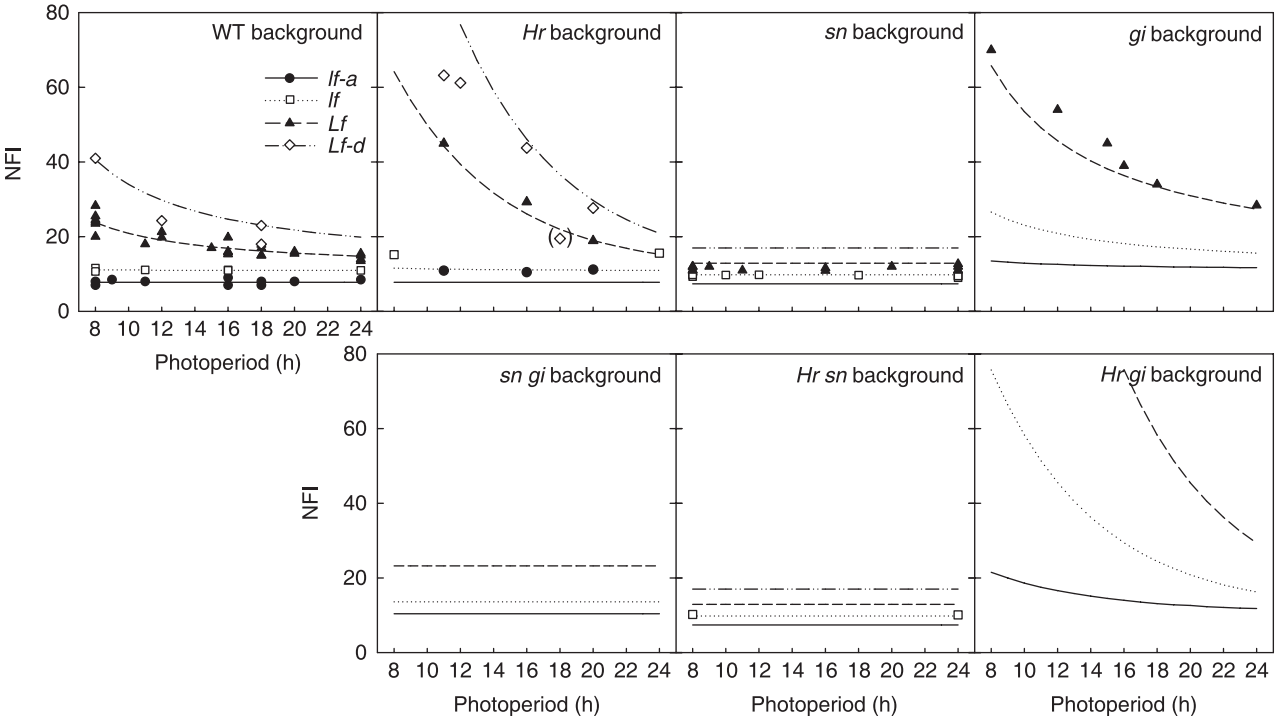

Fig. 4 Experimental and predicted data from the computational model for the node of flowering initiation (NFI) for different genotypes in different photoperiods [expressed in daily hours (h) of light]. Symbols represent the experimental data used to set the parameters and the lines represent the model predictions. Symbols in parentheses were not used for the optimization of parameters. WT has the genotype (*SN GI hr*). *GI*, *GIGAS*; *HR*, *HIGH RESPONSE TO PHOTOPERIOD*; *LF*, *LATE FLOWERING*; *SN*, *STERILE NODES*; WT, wild-type.

the RE is 14%. Variations for experimental data for each genotype and photoperiod condition can be up to 18% (*Lf* plants under an 8-h photoperiod). Consequently, with an RE of 9%, we consider the model predictions to be within an adequate range of error for the photoperiod conditions studied here.

Consistent with the experimental data for *hr sn* and *Hr sn* plants, predictions for *sn* mutants show no response to photoperiod. In addition, NFI predictions for *gi* mutants display a high response to photoperiod in an *Lf* background (Fig. 4), which accurately reproduces the experimental results. Model predictions also show that early lines corresponding to early *LF* alleles (*lf-a* and *lf*) on *hr* or *Hr* backgrounds do not respond to photoperiod, whereas late flowering genotypes (*Lf*, *Lf-d*) display a high response to photoperiod (Fig. 4). These flowering behaviours are observed in the experimental data.

Predictions for nonexisting allele combinations

No experimental results could be found in the literature for genotypes *sn Lf-d*, *sn gi* double mutants, *gi lf-a/lf/Lf-d* and *gi Hr*. Model outputs predict that *sn gi* double mutants are relatively late in comparison with *sn GI*, but do not respond to photoperiod (Fig. 4). In addition, for all *LF* alleles, *sn Hr* and *sn hr* plants are predicted to not respond to photoperiod. *gi* plants are predicted to initiate flowering very late, particularly in the *Hr* background where the photoperiod response is enhanced (Fig. 4).

Sensitivity of FS prediction to the synthesis and steady state of I

The change in I over time depends on the synthesis rate *r* and the steady-state I_∞. The range of flowering behaviours could be described by considering I_∞ as a constant. The model sensitivity to I_∞ was tested by varying the I_∞ value in wild-type plants in 24-h photoperiod conditions. As shown in Fig. S2a (see Supporting Information), the value for the constant I_∞, with the synthesis rate *r* kept constant, has a strong impact on FS. FS corresponds to the ratio of S to I (Eqn 4), and consequently the steady-state FS_∞ also depends on I_∞:

$$FS_\infty = \frac{S}{I_\infty} \qquad \text{Eqn 6}$$

For low I_∞ values (e.g. 0.05, Fig. S2a), the steady state FS_∞ is strongly increased. This results in a reduction in the time taken to reach this steady state. As expected, the model is highly sensitive to variations in I_∞, particularly for I_∞ values that are much lower than the initial condition I_0.

The constant K_R corresponds to the basal synthesis rate of I, *r*, set for the wild-type (*SN*, *hr*) in a 24-h photoperiod. When fitting the model to our experimental data, we found that *r* can vary with genotype and photoperiod, within the range 0.004–0.065. Over the considered range and, in particular, when K_R is close to zero, the values of K_R strongly impact on the rate at which FS reaches a steady-state value (FS_∞; Fig. S2b). Flower initiation is triggered when FS reaches the flowering threshold determined by *LF*. As shown in Fig. S2b, interactions between the rate at which FS reaches FS_∞ and these thresholds are highly correlated with NFI. In particular, for low K_R values (0.004–0.007, Fig. S2b), FS increases very slowly and never reaches *Lf* or *Lf-d* thresholds, which results in a vegetative state at the end of the simulation (80 nodes initiated at the apex, Fig. S2b).

To test how the model output would respond to different *r* values, the number of steps needed for FS to reach 95% of the steady-state value was calculated for different values of *r* (Fig. S2c). Consistent with preliminary results (Fig. S2b), the data indicate that FS predictions are highly sensitive to values of *r* below 0.1. These results are consistent with the differences observed between $\beta_{(SN,HR)}$(photoperiod) for *Hr* and *hr* genotypes. Values for $\beta_{(SN,HR)}$(photoperiod) in *Hr* genotypes under short-day photoperiods are very low and display a low slope, which results in a very low value of *r* (equivalent to K_R values of 0.004–0.013; Fig. S2b) and high values of NFI.

Sensitivity of NFI to β_{LF}

The sensitivity of the model predictions for NFI to the threshold parameter β_{LF} was analysed for different genotypes and photoperiods (Fig. S2d). All response curves converge towards the number of preformed nodes already initiated in the seed when β_{LF} is close to zero (Fig. S2d). This confirms that, when no threshold is present, flower initiation is triggered as soon as the plant germinates.

As shown in Fig. S2d, *gi* plants are more sensitive to changes in β_{LF} than *GI* plants (Fig. S2d). The model is highly sensitive to β_{LF} variation when β_{LF} is close to FS_∞ in value, suggesting a strong interaction. Consequently, the model sensitivity to variations in β_{LF} depends on S and I_∞. Comparison with experimental data indicated that the model-predicted NFI for late flowering plants on a mutant *gi* background was very sensitive to β_{LF} (Fig. S2d). By contrast, the model-predicted NFI for plants on a wild-type *GI* background was not sensitive to variations in β_{LF} (Fig. S2d). These results suggest that the model is strongly sensitive to parameter variations for late flowering phenotypes.

Discussion

Flowering has been extensively studied in pea through the identification and physiological analysis of mutants and wild-type lines showing variation in flowering time. These studies have led to the development of hypotheses about the genetic and physiological regulation of flowering in pea. The resulting flowering model, herein termed the 'classical' model, integrates the response to photoperiod and two mobile signals

(a flowering stimulus and a flowering inhibitor), and a threshold that the flowering signal (FS), defined as the ratio of a stimulus (S) to an inhibitor (I), must reach for flowering to occur. To test whether the classical model for flowering in pea was accurate and able to account for the wide range of experimental data, in addition to the prediction of new data, we developed a computational model based on these hypotheses and tested it against data collected from the literature and from experimental results presented here. As it currently allows the prediction of NFI for various genotypes and photoperiods, in the future, the model could be integrated into agronomic models to improve their capacity to predict yields in response to environmental conditions. In addition, improving the current model with new molecular data could provide a useful tool to test new hypotheses on the underlying mechanisms controlling flowering in pea. The molecular nature of the genes described in the model are just starting to be discovered (e.g., Foucher *et al.*, 2003; Hecht *et al.*, 2007; Weller, 2007). Future gene discoveries will enable better comparisons with other model species, such as *Arabidopsis*, and will lead to new experimental data and the development of new hypotheses to improve the model and our understanding of flowering control.

A simple formalism is sufficient to capture experimental data

The proposed model is based on our simplest expression of the classical hypothesis for flowering regulation in pea. In particular, the model includes a number of parameters and was fitted to the range of experimental data. To do so, some parameters were set arbitrarily, whereas others were set accordingly to fit the experimental data. This represented the most straightforward method of determining parameters. However, in the future, further experiments to provide more NFI data could allow a more accurate fitting of parameters. Sensitivity analyses suggested that β_{LF}, I_∞ and K_R had a strong impact on the model predictions of NFI. For instance, although NFI predictions were shown to be robust within a certain range of β_{LF} values, the model was highly sensitive to variations when values for β_{LF} were close to the steady state for FS. Consequently, high variations observed for NFI predictions in conditions in which the steady state for FS was close to β_{LF} might result from the model construction rather than from the actual biological mechanism. This, in addition to testing the $\beta_{(SN,HR)}$(photoperiod) functions, will require more biological data to improve the accuracy of parameter values.

Although the computational model will need to be tested against new experimental data, the predictions of NFI of existing genotype and photoperiod data are very satisfactory. We showed that a simple linear function could accurately predict that late flowering lines (*hr Lf-d* and *hr Lf gi* genotypes) display an enhanced response to photoperiod. Model predictions for *sn*, *dne* and *ppd* mutants are consistent with the experimental results (Fig. 4), supporting the concept that the photoperiod and flowering inhibitor (I) pathway interact (Fig. 1a). Predictions for *Hr* genotypes accurately capture experimental data (Fig. 4), suggesting that *HR* indeed has a role in the photoperiod response. However, because the photoperiod still affects the flowering node in *hr* mutants, in both the model and experimentally, it could be hypothesized that *HR* somehow enhances the effect of photoperiod, but is not necessary for a photoperiod response. New molecular data, in particular molecular characterization of the pea genes involved, should help us to further develop an understanding of the photoperiod pathway and how *HR* acts on this pathway and hence on flowering regulation.

Because the true nature of the signals involved in the regulation of flowering have not been identified, their quantification and modes of action were hypothesized. In particular, we hypothesized that the level of I would change over time, as suggested by Murfet & Reid (1973). Changes were a result of the simulated level of I displaying a sigmoid evolution over time, tending to a steady state I_∞. In addition, the stimulus level was considered to be constant over time and to depend only on the genotype for *GI*. Based on this construction, the level of FS changes over time towards a steady state, FS_∞. In the case in which FS_∞ is lower than the flowering threshold, the model predicts that certain genotypes should remain vegetative (for example, *gi Lf-d*; data not shown). This is supported by observations that some genotypes do not flower in some conditions (Beveridge & Murfet, 1996).

Observations that early flowering genotypes do not respond to photoperiod led to the hypothesis that these lines transition to flowering during a developmental stage at which the plant is not sensitive to photoperiod. In the computational model, we chose to define the photoperiod-insensitive phase as the period before the first true leaf at node 3 is open. However, estimations of the number of initiated primordia at the apex at this time point show that the number of nodes initiated at the apex, before the first leaf is open, displays a statistically significant response to photoperiod, but with no obvious trend. These results indicate that the photoperiod insensitivity phase might be shorter than expected in some conditions. Experiments in which plants are transferred from long-day to short-day photoperiods, and further studies on phytochrome light receptors, will be necessary to determine the duration of this photoperiod-insensitive phase.

Because most of the existing experimental data were reported as NFI (for example, Murfet, 1971c, 1973; Alcalde *et al.*, 2000), the computational model used 0.1 plastochron as the unit of time (where a plastochron is the time taken to initiate a new node). This is based on the assumption that the level of the signals could be expressed as a function of the number of nodes. The number of nodes is a function of thermal time rather than the calendar age of the plant (Collins & Wilson, 1974). Using the nodes as a time interval assumes

that temperature similarly influences the synthesis rate of I and the rate of node initiation. However, the hypothesis that NFI is independent of temperature arose from observations performed under field conditions (Truong & Duthion, 1993); this should be further evaluated by experiments in controlled conditions with a wide range of temperature × photoperiod combinations. In particular, if the temperature is shown to differentially affect the rate of node initiation and the synthesis rate of I, the model could be enhanced by incorporating temperature into the ordinary differential equation for I, together with an equation describing the temperature influence on the node initiation rate.

The computational model predicts NFI for nonexisting allele combinations

In addition to accurately predicting NFI for known genotypes, we used the computational model to predict NFI for allele combinations that have not been tested previously. For example, *sn* mutations combined with late alleles, including *Lf-d* and *Hr*, should not respond to photoperiod, but should exhibit a later flowering phenotype compared with single *sn* mutants (Fig. 4). As *SN* is hypothesized to be necessary for photoperiod response, inhibition of photoperiod response in *sn* double mutants is expected. In a wild-type *SN* background, early *LF* genotypes (*lf-a*, *lf*) do not respond to photoperiod, whereas late genotypes are characterized by a high photoperiod response (Fig. 4). Accordingly, experimental results for *sn* mutants indicate that the absence of photoperiod response could be linked exclusively to their early phenotype, instead of an effective inhibition of photoperiod response. Consequently, further experimental results for *sn* mutants associated with late alleles will be necessary to test whether the model predictions capture the role for the *SN* gene product. In addition, future studies to ascertain NFI for these and other nonexisting allele combinations will allow the testing of whether the model predictions are consistent with experimental data.

Applications of the current model

For agronomic purposes, the manipulation of the flowering time is essential to develop improved pea cultivars. With a better understanding and prediction of flowering time, new 'virtual' pea genotypes could be constructed and their flowering phenotypes predicted under different environmental conditions (Lejeune-Hénaut *et al.*, 1999, 2008). The development of winter pea cultivars is necessary to improve pea crop productivity (Lejeune-Hénaut *et al.*, 2008). For winter pea crops, the manipulation of flowering regulatory genes appears to be a promising way to control key developmental stages, such as the dates of floral initiation and flowering. An ideal winter pea should initiate its flower primordia sufficiently late to avoid winter frosts, but flower sufficiently early to escape drought and heat stresses in late spring. The current strategy is to combine the dominant *HR* allele, which confers high response to short-day photoperiods, with an appropriate allele of *LF*. A good combination of alleles should allow an ideal flowering time in the ideal winter pea candidates.

The computational model presented here allowed the prediction of NFI for different allele combinations for *HR* and *LF*, which are essential components of the winter pea breeding strategy. By combining our computational model with the calculation of leaf initiation and appearance in thermal time, such as that introduced by Truong & Duthion (1993), the prediction of NFI could be integrated into a crop model to quantitatively predict the time of flower initiation. This could be performed for virtual candidate genotypes under a range of different climates, allowing breeders to choose ideal allele combinations that give their desired flowering time and environmental responses.

However, for agronomic purposes, it is essential to also consider flower development from initiation to opening, as fully developed flowers are key factors for yield. Therefore, it will be necessary to study, and later include in the computational model, floral abortion and the time that flowers take to develop. This will allow the accurate prediction of the flowering node and time under different photoperiod conditions. Currently, the computational model can be simulated for constant photoperiods; new biological and modelling experiments are needed to test whether the model allows the accurate prediction of the flowering node under changing photoperiods, similar to field conditions. It may be necessary to alter the model to integrate the response to natural changes in photoperiod.

Perspectives for improving the flowering model

New hypotheses, derived from emerging molecular data, should allow more accurate modelling of flowering regulation in pea. This will allow us to explicitly describe underlying mechanisms and to integrate molecular, genetic and physiological data. Molecular analyses of flowering in pea have been, and will continue to be, accelerated by the extensive work in *Arabidopsis*, together with the development of sequence databases for model legumes and the well-documented synteny between pea and *Medicago* (Zhu *et al.*, 2005; Aubert *et al.*, 2006).

Currently, the best option to improve our understanding of flowering control in pea is to compare new results in pea with what is well known in other model species. Mechanisms that control the timing of flower initiation have been extensively studied in *Arabidopsis*. The isolation of new photoperiod response mutants and *Arabidopsis* photoperiod pathway gene homologues in pea suggests that the regulation of flowering in pea is very similar to that in *Arabidopsis* (Hecht *et al.*, 2005, 2007). Notably, the *LF* locus, which was the first of the classical pea flowering loci to be identified at the molecular level, was shown to be homologous to the *Arabidopsis* flowering

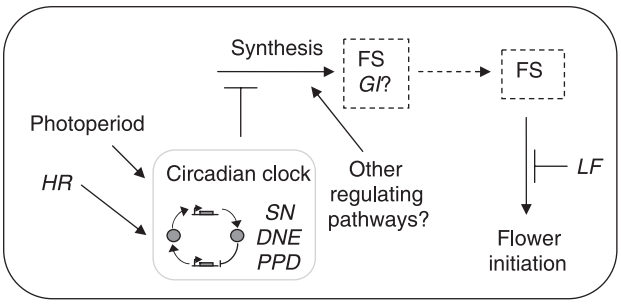

Fig. 5 New conceptual model for the regulation of flowering in pea (*Pisum sativum*). The synthesis of a putative mobile flowering signal (FS) is under genetic and photoperiodic control via the circadian clock. Flowering is triggered when FS exceeds a certain threshold defined by the different alleles of *LF*. Mobile signals are shown as broken lines, and genes are given in italic. Arrowheads indicate a promotion, and flat-ended lines represent repression. *DNE*, *DIE NEUTRALIS*; *GI*, *GIGAS*; *HR*, *HIGH RESPONSE TO PHOTOPERIOD*; *LF*, *LATE FLOWERING*; *PPD*, *PHOTOPERIOD*; *SN*, *STERILE NODES*.

inhibitor gene *TERMINAL FLOWER1* (*TFL1*) (Foucher *et al.*, 2003). In the classical model for flowering control in pea, the flowering threshold is determined by the different alleles of *LF*. Recent discoveries in *Arabidopsis* suggest a molecular mechanism for this threshold. TFL1 is a repressor of flowering and is homologous to *FLOWERING LOCUS T* (*FT*), a key target and integrator of several flowering pathways, including photoperiod, vernalization and gibberellins. FT and TFL1 proteins are similar in structure, except in a few regions (Hanzawa *et al.*, 2005). FT and TFL1 do not interact with each other, but do interact antagonistically with the protein FLOWERING LOCUS D (FD) (Abe *et al.*, 2005; Wigge *et al.*, 2005; Ahn *et al.*, 2006). When interacting with TFL1, FD inhibits flowering, whereas its interaction with FT activates flowering (Wigge *et al.*, 2005). Antagonism between FT and TFL1 implies that, the higher the level of TFL1 at the apex, the higher the level of FT that is needed to overcome the TFL1/FD inhibition to trigger flowering initiation. Accordingly, the level of TFL1 at the apex represents a flowering threshold for the flowering signal (Ahn *et al.*, 2006). This model for interaction of FD with FT and TFL1 led to the hypothesis that the abundance of TFL1 can be seen as a threshold for flowering initiation. A similar mechanism may explain the role of *LF* in determining a threshold level for flowering in pea. Further investigation will allow for a more accurate modelling of this *LF* effect.

The pea *GI* gene was found to colocalize in the region of an *FT* cluster. This supports the hypothesized role of *GI* as a flowering promoter (Hecht *et al.*, 2005). Molecular characterization of *GI* will allow the quantification of its product during development, and testing of the model hypothesis that the level of the flowering stimulus is constant over time in pea.

The photoperiod response in pea involves rhythmic regulation by the circadian clock via mechanisms similar to those in rice and *Arabidopsis* (Hecht *et al.*, 2007; Kobayashi & Weigel, 2007; Tamaki *et al.*, 2007; Weller, 2007). This was not included in our computational model because the molecular data in pea are currently not sufficient to develop such a computational model. Future studies should incorporate such mechanisms when sufficient data are available.

Future computational models of the regulation of flowering in pea might consider whether the circadian clock affects the flowering signal as it affects *FT* in *Arabidopsis*. In such a model, the production of the flowering signal would be reduced in unfavourable day length conditions by a mechanism controlled by the circadian clock (Fig. 5). These new hypotheses will require new equations to describe the regulation of the flowering signal by photoperiod. This should be integrated into the model in the future when sufficient molecular data are available to build such a model. In such a model, the flowering signal would accumulate over time, independent of the node appearance rate. When it reached a flowering threshold determined by the *LF* allele, equivalent to the classical model threshold, flower initiation would be triggered. Further molecular experiments will be necessary to identify and quantify the flowering signal, together with its regulation by the circadian clock. The ongoing identification of pea circadian clock genes (Hecht *et al.*, 2007) and their expression levels under different photoperiod conditions should lead to a better understanding of the control of photoperiod response by the circadian clock.

In this study, the 'classical' hypothesis was incorporated into a quantitative model that improved our ability to accurately test hypotheses against observations. We found that our hypotheses could accurately explain NFI data for many different genotypes grown in different photoperiods. As a first modelling attempt, this work has opened up a number of avenues for modelling genetic control of developmental processes in pea.

Acknowledgements

This work was supported by INRA (B.W.). The authors thank Jean-Paul Pillot for technical assistance and the two anonymous reviewers for helpful comments.

References

Abe M, Kobayashi Y, Yamamoto S, Daimon Y, Yamaguchi A, Ikeda Y, Ichinoki H, Notaguchi M, Goto K, Araki T. 2005. FD, a bZIP proteinmediating signals from the floral pathway integrator FT at the shoot apex. *Science* **309**: 1052–1056.

Ahn JH, Miller D, Winter VJ, Banfield MJ, Lee JH, Yoo SY, Henz SR, Brady RL, Weigel D. 2006. A divergent external loop confers antagonistic activity on floral regulators FT and TFL1. *The EMBO Journal* **25**: 605–614.

Alcalde J, Wheeler T, Summerfield R. 1999a. Flowering genes and the photothermal flowering responses of pea (*Pisum sativum*): a re-analysis. *Australian Journal of Plant Physiology* **26**: 379–386.

Alcalde J, Wheeler T, Summerfield R, Norero A. 1999b. Quantitative effects of the genes *LF*, *SN*, *E*, and *HR* on time to flowering in pea (*Pisum sativum* L.). *Journal of Experimental Botany* **50**: 1691–1700.

Alcalde JA, Wheeler TR, Summerfield RJ. 2000. Genetic characterization of flowering of diverse cultivars of pea. *Agronomy Journal* **92**: 772–779.

Arumingtyas EL, Murfet I. 1994. Flowering in *Pisum*: a further gene controlling response to photoperiod. *Journal of Heredity* **85**: 12–17.

Aubert G, Morin J, Jacquin F, Loridon K, Quillet MC, Petit A, Rameau C, Lejeune-Henaut I, Huguet T, Burstin J. 2006. Functional mapping in pea, as an aid to the candidate gene selection and for investigating synteny with the model legume *Medicago truncatula*. *Theoretical and Applied Genetics* **112**: 1024–1041.

Barber HN, Paton DM. 1952. A gene controlled flowering inhibitor in *Pisum*. *Nature* **169**: 592.

Bayliss WM. 1902. On the local reactions of the arterial wall to changes in internal pressure. *Journal of Physiology* **28**: 220–231.

Berry GJ, Aitken Y. 1979. Effect of photoperiod and temperature on flowering in pea (*Pisum sativum* L.). *Australian Journal of Plant Physiology* **6**: 573–587.

Beveridge CA, Murfet IC. 1996. The *gigas* mutant in pea is deficient in the floral stimulus. *Physiologia Plantarum* **96**: 637–645.

Boss PK, Bastow RM, Mylne JS, Dean C. 2004. Multiple pathways in the decision to flower: enabling, promoting, and resetting. *Plant Cell* **16**: S18–S31.

Chaos Á, Aldana M, Espinosa-Soto C, de León BGP, Alvarez-Buylla ER. 2006. From genes to flower patterns and evolution: dynamic models of gene regulatory networks. *Journal of Plant Growth Regulation* **25**: 278–289.

Colasanti J, Sundaresan V. 2000. 'Florigen' enters the molecular age: long-distance signals that cause plants to flower. *Trends in Biochemical Sciences* **25**: 236–240.

Collins WJ, Wilson JH. 1974. Node of flowering as an index of plant development. *Annals of Botany* **38**: 175–180.

Collinson ST, Ellis RH, Summerfield S, Roberts EH. 1992. Durations of the photoperiod-sensitive and photoperiod-insensitive phases of development to flowering in four cultivars of rice (*Oryza sativa* L.). *Annals of Botany* **70**: 339–346.

Espinosa-Soto C, Padilla-Longoria P, Alvarez-Buylla ER. 2004. A gene regulatory network model for cell-fate determination during *Arabidopsis thaliana* flower development that is robust and recovers experimental gene expression profiles. *Plant Cell* **16**: 2923–2939.

Foucher F, Morin J, Courtiade J, Cadioux S, Ellis N, Banfield MJ, Rameau C. 2003. *DETERMINATE* and *LATE FLOWERING* are two *TERMINAL FLOWER1/CENTRORADIALIS* homologs that control two distinct phases of flowering initiation and development in pea. *Plant Cell* **15**: 2742–2754.

Hanzawa Y, Money T, Bradley D. 2005. A single amino acid converts a repressor to an activator of flowering. *Proceedings of the National Academy of Sciences, USA* **102**: 7748–7753.

Haupt W. 1969. *Pisum sativum* L. In: Evans LT, ed. *The induction of flowering*. Melbourne, Australia: Macmillan, 393–408.

Hecht V, Foucher F, Ferrandiz C, Macknight R, Navarro C, Morin J, Vardy ME, Ellis N, Beltran JP, Rameau C *et al.* 2005. Conservation of Arabidopsis flowering genes in model legumes. *Plant Physiology* **137**: 1420–1434.

Hecht V, Knowles CL, Vander Schoor JK, Liew LC, Jones SE, Lambert MJ, Weller JL. 2007. Pea *LATE BLOOMER1* is a *GIGANTEA* ortholog with roles in photoperiodic flowering, deetiolation, and transcriptional regulation of circadian clock gene homologs. *Plant Physiology* **144**: 648–661.

Heisler MG, Jönsson H. 2006. Modeling auxin transport and plant development. *Journal of Plant Growth Regulation* **25**: 302–312.

King WM, Murfet IC. 1985. Flowering in *Pisum*: a sixth locus, dne. *Annals of Botany* **56**: 835–846.

Kobayashi Y, Weigel D. 2007. Move on up, it's time for change – mobile signals controlling photoperiod-dependent flowering. *Genes and Development* **21**: 2371–2384.

Kramer EM. 2006. Wood grain pattern formation: a brief overview. *Journal of Plant Growth Regulation* **25**: 290–301.

Lang A, Chailakhyan MK, Frolova IA. 1977. Promotion and inhibition of flower formation in a dayneutral plant in grafts with a short-day plant and a long-day plant. *Proceedings of the National Academy of Sciences, USA* **74**: 2412–2416.

Lejeune-Hénaut I, Bourion V, Etévé G, Cunot E, Delhaye K, Demyter C. 1999. Floral initiation in field-grown forage peas is delayed to a greater extent by short photoperiods, than in other types of European varieties. *Euphytica* **109**: 201–211.

Lejeune-Hénaut I, Hanocq E, Bethencourt L, Fontaine V, Delbreil B, Morin J, Petit A, Devaux R, Boilleau M, Stempniak JJ *et al.* 2008. The flowering locus *HR* colocalizes with a major QTL affecting winter frost tolerance in *Pisum sativum* L. *Theoretical and Applied Genetics* **116**: 1105–1116.

Lester DR, Mackenzie-Hose AK, Davies PJ, Ross JJ, Reid JB. 1999. The influence of the null *le-2* mutation on gibberellin levels in developing pea seeds. *Plant Growth Regulation* **27**: 83–89.

Locke JC, Millar AJ, Turner MS. 2005. Modelling genetic networks with noisy and varied experimental data: the circadian clock in *Arabidopsis thaliana*. *Journal of Theoretical Biology* **234**: 383–393.

Maurer AR, Jaffray DE, Fletcher HF. 1966. Responses of peas to environment III. Assessment of the morphological development of peas. *Canadian Journal of Plant Science* **46**: 285–290.

Mendoza L, Alvarez-Buylla ER. 2000. Genetic regulation of root hair development in *Arabidopsis thaliana*: A network model. *Journal of Theoretical Biology* **204**: 311–326.

Mendoza L, Thieffry D, Alvarez-Buylla ER. 1999. Genetic control of flower morphogenesis in *Arabidopsis thaliana*: a logical analysis. *Bioinformatics* **15**: 593–606.

Murfet IC. 1971a. Flowering in *Pisum*. A three-gene system. *Heredity* **27**: 93–110.

Murfet IC. 1971b. Flowering in *Pisum*. Three distinct phenotypic classes determined by the interaction of a dominant early and a dominant late gene. *Heredity* **26**: 243–257.

Murfet IC. 1971c. Flowering in *Pisum*: Reciprocal grafts between known genotypes. *Australian Journal of Biological Sciences* **24**: 1089–1101.

Murfet IC. 1973. Flowering in *Pisum*. *HR*, a gene for high response to photoperiod. *Heredity* **31**: 157–164.

Murfet I. 1975. Flowering in *Pisum*: multiple alleles at the *LF* locus. *Heredity* **35**: 85–98.

Murfet IC. 1977. The physiological genetics of flowering. In: Sutcliffe JF, Pate JS, eds. *The physiology of the garden pea*. Academic Press, London, UK, pp. 385–430.

Murfet IC. 1989. Flowering genes in *Pisum*. In: Lord EM, Bernier G, eds. *Plant Reproduction: From Floral Induction to Pollination*. American Society of Plant Physiologists, Rockville, MD, USA, pp. 10–18.

Murfet IC, Reid JB. 1973. Flowering in *Pisum*: evidence that gene SN controls a graft-transmissible inhibitor. *Australian Journal of Biological Sciences* **26**: 675–677.

Murfet I, Reid JB. 1993. Developmental mutants. In: Casey R, Davies DR, eds. *Peas: genetics, molecular biology and biotechnology*. Wallingford, UK: CAB International.

Reid JB. 1979. Flowering in *Pisum*: the effect of age on the gene *SN* and the site of action of gene *HR*. *Annals of Botany* **44**: 163–173.

Reid JB, Murfet IC, Singer SR, Weller JL, Taylor SA. 1996. Physiological-genetics of flowering in *Pisum*. *Seminars in Cell and Developmental Biology* **7**: 455–463.

Tamaki S, Matsuo S, Wong HL, Yokoi S, Shimamoto K. 2007. Hd3a protein is a mobile flowering signal in rice. *Science* **316**: 1033–1036.

Taylor S, Murfet I. 1993. Flowering in pea: a mutation from *Lfd* to *lfa* and a summary of induced *LF* mutations. *Pisum Genetics* **25**: 60–63.

Taylor SA, Murfet I. 1996. Flowering in *Pisum*: identification of a new *ppd* allele and its physiological action as revealed by grafting. *Physiologia Plantarum* **97**: 719–723.

Truong HH, Duthion C. 1993. Time of flowering of pea (*Pisum sativum* L.) as a function of leaf appearance rate and node of first flower. *Annals of Botany (Lond)* **72**: 133–142.

Welch SM, Roe JL, Dong Z. 2003. A genetic neural network model of flowering time control in *Arabidopsis thaliana*. *Agronomy Journal* **95**: 71–81.

Weller JL. 2007. Update on the genetics of flowering. *Pisum Genetics* **39**: 1–8.

Weller JL, Reid JB, Taylor SA, Murfet IC. 1997. The genetic control of flowering in pea. *Trends in Plant Science* **2**: 412–418.

Wigge PA, Kim MC, Jaeger KE, Busch W, Schmid M, Lohmann JU, Weigel D. 2005 Integration of spatial and temporal information during floral induction in Arabidopsis. *Science* **309**: 1056–1059.

Zhu H, Choi HK, Cook DR, Shoemaker RC. 2005. Bridging model and crop legumes through comparative genomics. *Plant Physiology* **137**: 1189–1196.

Supporting Information

Additional Supporting Information may be found in the online version of this article:

Fig. S1 Number of nodes initiated at the apex and open leaves on the main stem vs thermal time, expressed in cumulative degree-days, from sowing for NGB5839 plants grown in a glasshouse under an 11-h photoperiod.

Fig. S2 Sensitivity of the flowering signal (FS) and node of flower initiation (NFI) predictions to parameter variation.

Table S1 Genotype of each line used in the experiments in this study

Table S2 Number of preformed nodes observed in seeds for different genotypes and harvests

Table S3 Node of flowering initiation (NFI) for different genotypes obtained from previous studies

Table S4 Node of flowering initiation (NFI) for each genotype grown in 11, 16 and 20-h photoperiods in a glasshouse

Table S5 Estimation of the number of nodes initiated at the apex when the first true leaf (node 3) is open

Please note: Wiley-Blackwell are not responsible for the content or functionality of any supporting materials supplied by the authors. Any queries (other than missing material) should be directed to the corresponding author for the article.